

Supplementary Materials

Comparing Internal and Interparticle Space Effects of Metal–Organic Frameworks on Polysulfide Migration in Lithium–Sulfur Batteries

UnJin Ryu ¹, Won Ho Choi ², Panpan Dong ³, Jeeyoung Shin ^{2,4,*}, Min-Kyu Song ^{3,*} and Kyung Min Choi ^{1,2,5,*}

¹ Industry Collaboration Center, Sookmyung Women's University, Cheongpa-ro 47-gil 100, Yongsan-gu, Seoul 04310, Korea; unjin@sookmyung.ac.kr

² Institute of Advanced Materials and Systems, Sookmyung Women's University, Cheongpa-ro 47-gil 100, Yongsan-gu, Seoul 04310, Korea; wonhochoi@sookmyung.ac.kr

³ School of Mechanical and Materials Engineering, Washington State University, Pullman, WA 99164, USA; panpan.dong@wsu.edu

⁴ Department of Mechanical Systems Engineering, Sookmyung Women's University, Cheongpa-ro 47-gil 100, Yongsan-gu, Seoul 04310, Korea

⁵ Department of Chemical and Biological Engineering, Sookmyung Women's University, Cheongpa-ro 47-gil 100, Yongsan-gu, Seoul 04310, Korea

* Correspondence: jshin@sookmyung.ac.kr(J.S.); minkyu.song@wsu.edu (M.-K.S.); kmchoi@sookmyung.ac.kr (K.M.C.)

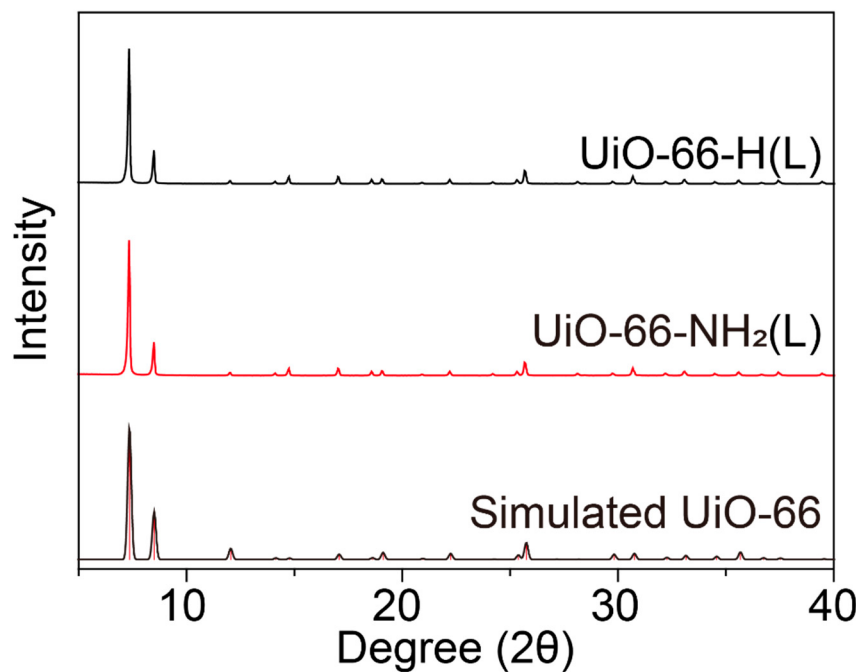


Figure S1. PXRD patterns of simulated UiO-66, UiO-66-H(L), and UiO-66-NH₂(L).

	Li ₂ S ₆	UiO-66-H			UiO-66-NH ₂			Li ₂ S ₆	UiO-66-H			UiO-66-NH ₂			
		(L)	(M)	(S)	(L)	(M)	(S)		(L)	(M)	(S)	(L)	(M)	(S)	
After 0 h				After 6 h											
After 1 h				After 8 h											
After 2 h				After 10 h											
After 4 h				Supernatant											

Figure S2. Digital images of 4 mM Li₂S₆ solution before and after soaking UiO-66s powders for 10 h for visual analysis of absorption.

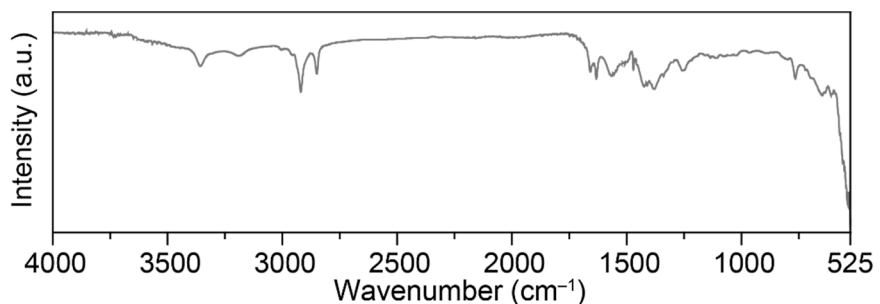


Figure S3. FT-IR spectra of Li₂S₆ solution after drying on a diamond ATR plate.

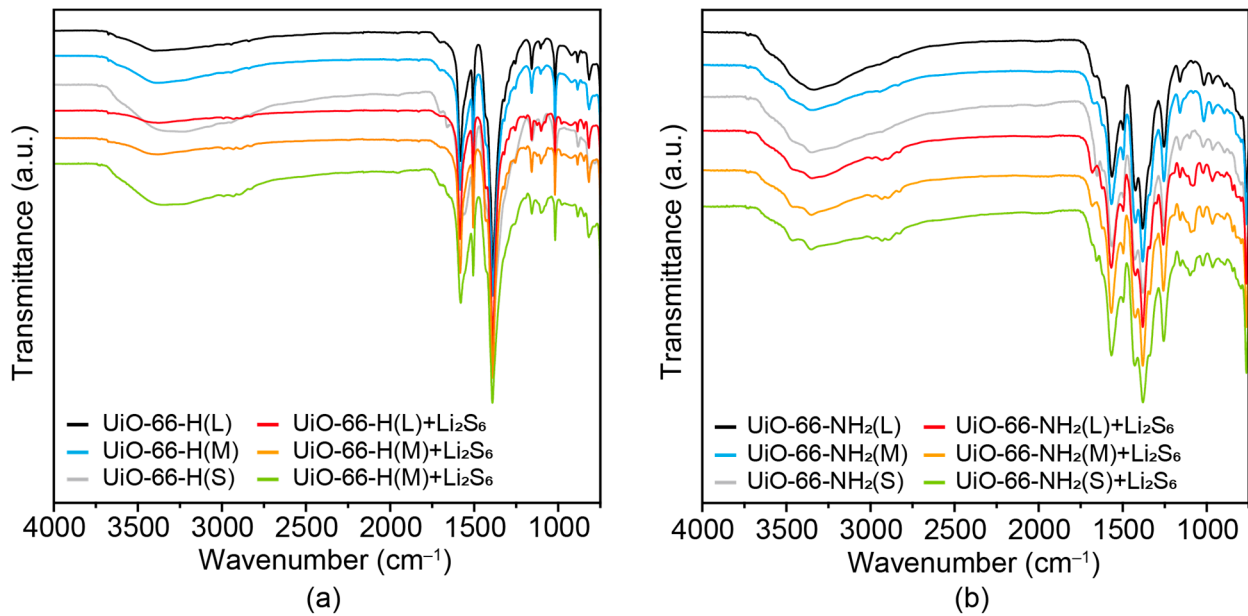


Figure S4. (a) FT-IR spectra of UiO-66-H(X) before and after absorbing polysulfide at 750–4,000 cm^{-1} . (b) FT-IR spectra of UiO-66-NH₂(X) before and after absorbing polysulfide at 750–4,000 cm^{-1} .

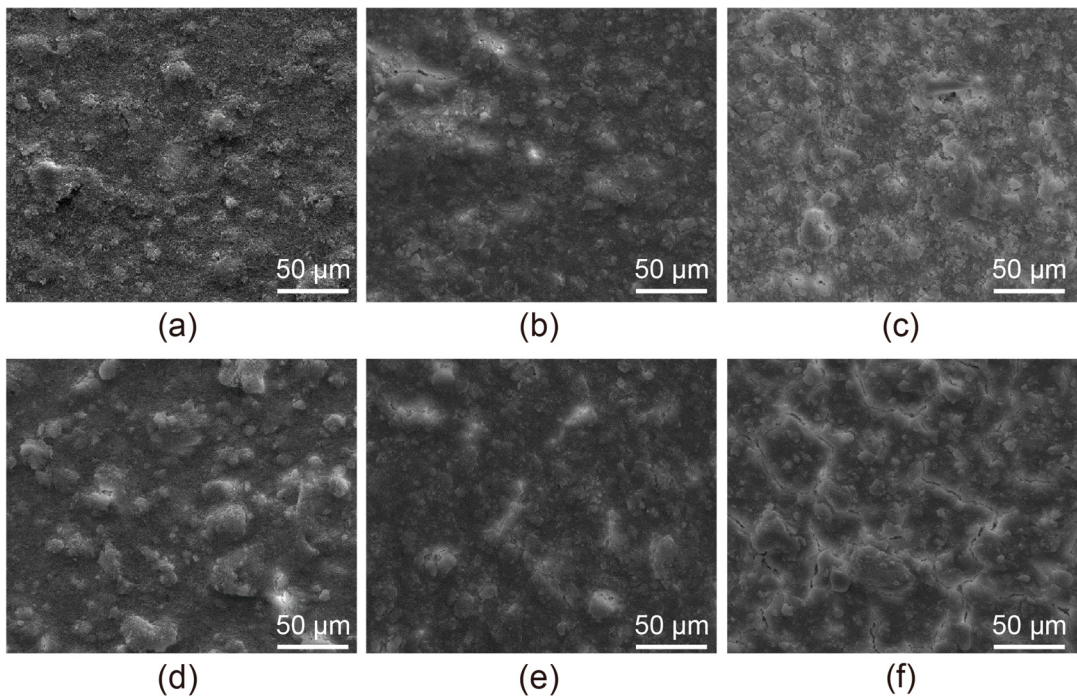


Figure S5. SEM images of the surface of MOF-coated separators made of (a) UiO-66-H(L), (b) UiO-66-H(M), (c) UiO-66-H(S), (d) UiO-66-NH₂(L), (e) UiO-66-NH₂(M), and (f) UiO-66-NH₂(S).

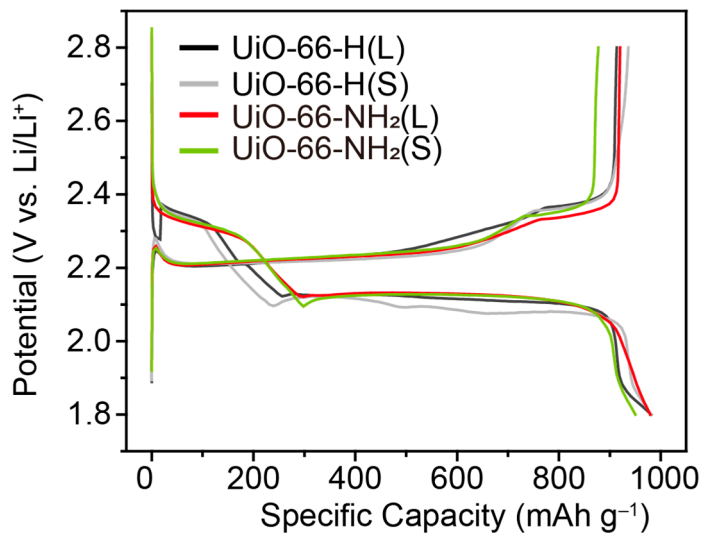


Figure S6. Voltage profiles of UiO-66-H(S),(L) , and $\text{UiO-66-NH}_2\text{(S),(L)}$ tested under 100 mA g^{-1} .

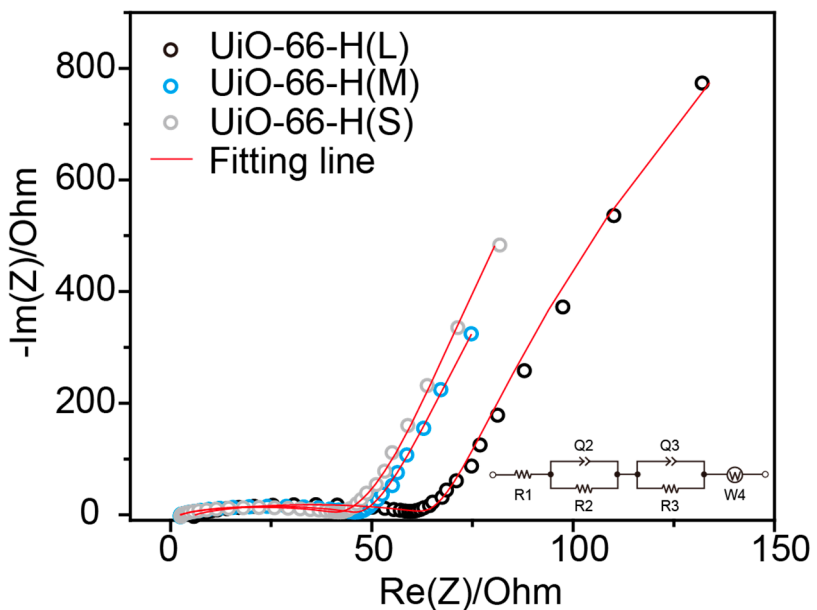


Figure S7. Nyquist plots of fresh Li-S cells with $\text{UiO-66-H}(X)$ coated separators.

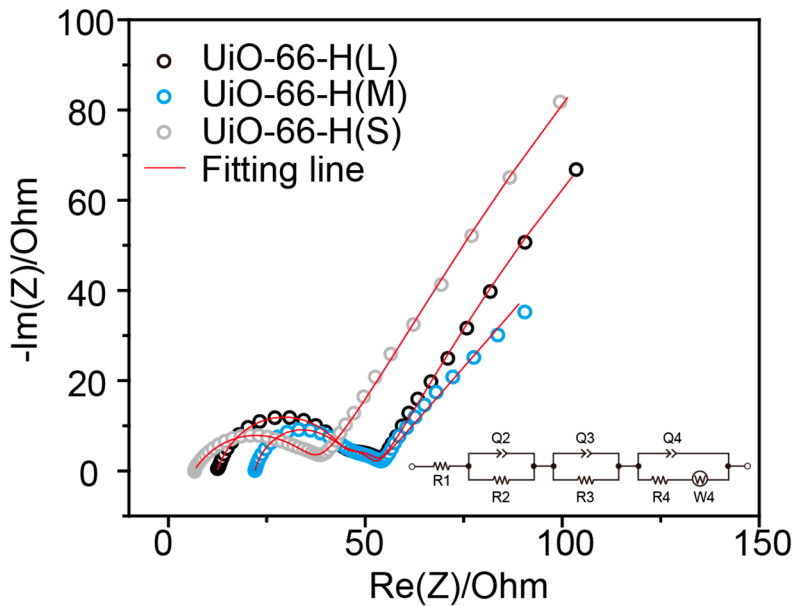


Figure S8. Nyquist plots of Li–S cells after 350 cycles with $\text{UiO-66-H}(X)$ -coated separators.

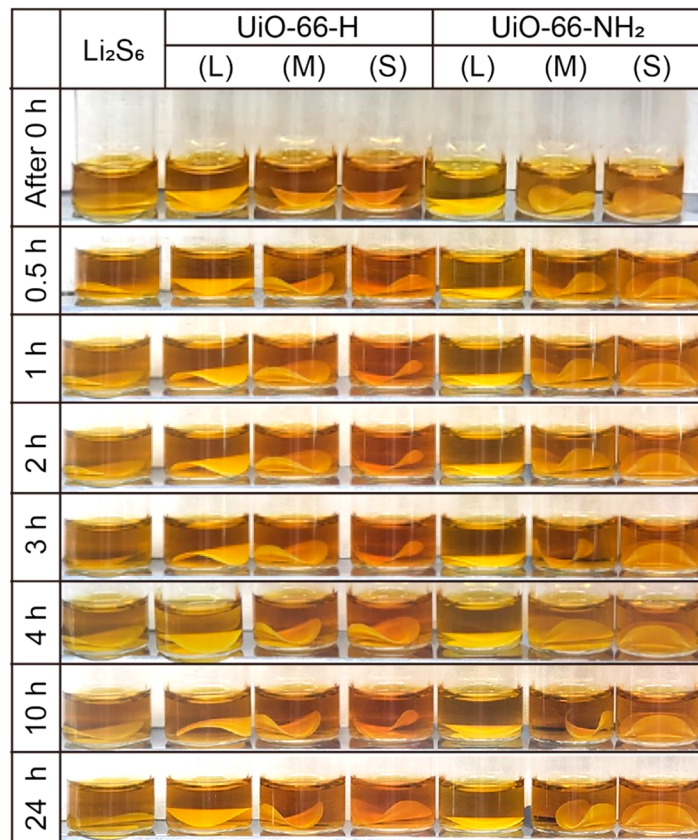


Figure S9. Digital images of Li_2S_6 solution before and after soaking MOF-coated separators for 24 h for visual analysis of absorption.

Table S1. Pore structure parameters of UiO-66s.

Sample	S_{BET} ¹ ($\text{m}^2 \text{g}^{-1}$)	V_p ¹ ($\text{cm}^3 \text{g}^{-1}$)	d_p ² (nm)
UiO-66-H(L)	1292.8	0.5182	0.6
UiO-66-H(M)	1094.2	0.5804	0.6
UiO-66-H(S)	1091.7	1.0913	0.6
UiO-66-NH ₂ (L)	1040	0.4786	0.6
UiO-66-NH ₂ (M)	1024.9	0.7475	0.6
UiO-66-NH ₂ (S)	766.97	1.0259	0.6

¹ S_{BET} (BET surface area) and V_p (pore volume) were calculated by BET analysis.² d_p (pore diameter) were calculated by MP plot.**Table S2.** The comparison of electrochemical performance of reported UiO-66 coated separators in Li–S batteries.

MOFs	Separator substrate	Cathode materials	Mass loading of S (mg/cm^2)	Electrolyte (1/1, v/v)	C-rate	Cycle number	Ref.
UiO-66-H	Celgard 2500	S/Super P	1.5	1M LiTFSI in DOL/DME (1C=1675 mA g ⁻¹)	0.2C (1C=1675 mA g ⁻¹)	720 mAh g ⁻¹ @500 cycles	[1]
UiO-66-H	Carbon cloth	S/CNT	2.1	1M LiTFSI in DOL/DME with 0.1M Li ₂ S ₈ (1C=1675 mA g ⁻¹)	1C (1C=1675 mA g ⁻¹)	600 mAh g ⁻¹ after 600 cycles	[2]
UiO-66-S ¹	Polyethylene membrane	S/rGO	1.7	1M LiTFSI in DOL/DME (1C=1672 mA g ⁻¹)	0.2C (1C=1672 mA g ⁻¹)	437.6 mAh g ⁻¹ @200 cycles	[3]
UiO-66-SO ₃ Li	Free-standing	S/CMK-3	2.0	1M LiTFSI in DOL/DME with 2wt% LiNO ₃ (1C=1675 mA g ⁻¹)	0.5C (1C=1675 mA g ⁻¹)	500 mAh g ⁻¹ @500 cycles	[4]
UiO-66-NH ₂ @SiO ₂	Celgard 2320	S/graphene	0.5	1M LiTFSI in DOL/TEGDME (1C=1672 mA g ⁻¹)	0.1C (1C=1672 mA g ⁻¹)	600 mAh g ⁻¹ @100 cycles	[5]
UiO-66-NH ₂ @graphene	GF	S/CNT	1.4	1M LiTFSI in DOL/DME with 1wt% LiNO ₃ (1C=1675 mA g ⁻¹)	1C (1C=1675 mA g ⁻¹)	500 mAh g ⁻¹ after 500 cycles	[6]
UiO-66-H (L); UiO-66-NH ₂ (L)	Celgard 2400	S/CNT	0.6-1.0	1M LiTFSI in DOL/DME with 0.2M LiNO ₃ (1C=1675 mA g ⁻¹)	0.15C (1C=1675 mA g ⁻¹)	271 mAh g ⁻¹ after 350 cycles; 420 mAh g ⁻¹ after 350 cycles	This work

¹ Sulfonic-acid functionalized UiO-66.

Table S3. EIS fitting parameters of fresh Li–S cells with UiO-66-H(X) coated separators.

	UiO-66-H(L)	UiO-66-H(M)	UiO-66-H(S)
R1 (Ω)	6.14	2.474	2.585
Q2 ($F s^{a-1}$)	39.95e-6	26.71e-6	30.12e-6
a2	0.7162	0.7689	0.769
R2 (Ω)	56.3	43.21	38.06
Q3 ($F s^{a-1}$)	4.492e-3	5.198e-3	5.172e-3
a3	0.9886	0.9906	1.0
R3 (Ω)	18167	22314	27568
$Z_w (\Omega s^{1/2})$	14.76	16.28	21.35

Table S4. EIS fitting parameters of Li–S cells with UiO-66-H(X) coated separators after 350 cycles.

	UiO-66-H(L)	UiO-66-H(M)	UiO-66-H(S)
R1 (Ω)	12.43	21.97	6.521
Q2 ($F s^{a-1}$)	12.46e-6	8.829e-6	0.2231e-3
A2	0.7838	0.8417	0.6001
R2 (Ω)	33.1	22.0	29.7
Q3 ($F s^{a-1}$)	0.1794	11.18	0.1653
A3	0.7769	0.5173e-12	0.8
R3 (Ω)	221.1	231.5	298.6
Q4 ($F s^{a-1}$)	1.438e-3	0.5417e-3	0.04394
A4	0.8329	0.7862	0.458
R4 (Ω)	6.894	8.145	8.582
$Z_w (\Omega s^{1/2})$	6.906	9.265	29.93

References

1. Fan, Y.; Niu, Z.; Zhang, F.; Zhang, R.; Zhao, Y.; Lu, G. Suppressing the Shuttle Effect in Lithium–Sulfur Batteries by a UiO-66-Modified Polypropylene Separator. *ACS omega* **2019**, *4*, 10328, <https://doi.org/10.1021/acsomega.9b00884>.
2. Zheng, S.; Zhao, X.; Liu, G.; Wu, F.; Li, J. A multifunctional UiO-66@carbon interlayer as an efficacious suppressor of polysulfide shuttling for lithium–sulfur batteries. *Nanotechnology*, **2021**, *32*, 365404, <https://doi.org/10.1088/1361-6528/ac06f7>.
3. Kim, S.H.; Yeon, J.S.; Kim, R.; Choi, K.M.; Park, H.S. A functional separator coated with sulfonated metal–organic framework/Nafion hybrids for Li–S batteries. *J. Mater. Chem. A*, **2018**, *6*, 24971, <https://doi.org/10.1039/C8TA08843H..>
4. Wang, Z.; Huang, W.; Hua, J.; Wang, Y.; Yi, H.; Zhao, W.; Zhao, Q.; Jia, H.; Fei, B.; Pan, F. An Anionic-MOF-Based Bifunctional Separator for Regulating Lithium Deposition and Suppressing Polysulfides Shuttle in Li–S Batteries. *Small Methods* **2020**, *4*, 2000082, <https://doi.org/10.1002/smtd.202000082>.
5. Suriyakumar, S.; Stephan, A.M.; Angulakshmi, N.; Hassan, M.H.; Alkordi, M.H. Metal–organic framework@SiO₂ as permselective separator for lithium–sulfur batteries. *J. Mater. Chem. A*, **2018**, *6*, 14623, <https://doi.org/10.1039/C8TA02259C>.
6. Guo, S.; Xiao, Y.; Wang, J.; Ouyang, Y.; Li, X.; Deng, H.; He, W.; Zeng, Q.; Zhang, W.; Zhang, Q. Ordered structure of interlayer constructed with metal–organic frameworks improves the performance of lithium–sulfur batteries. *Nano Research*, **2021**, <https://doi.org/10.1007/s12274-021-3372-5>.